IRSTI 29.31.15 https://doi.org/10.26577/phst.2023.v10.i1.04

On the invasiveness of the electro-optical research method in strong inhomogeneous electric and light fields

V.B. Yassinskiy* and Yu.A. Kuznetsova

Abylkas Saginov Karaganda Technical University, Karaganda, Kazakhstan
*e-mail: yas@inbox.ru

(Received March 13, 2023; received in revised form May 03, 2023; accepted May 23, 2023)

Optical research methods are usually considered non-invasive, that is, they do not affect the object of study. However, under certain conditions, this is not the case. In the article, as a result of comparing experimental and calculated kerrograms, it is shown that during electro-optical measurements in nitrobenzene using the Kerr effect, a strong electric field and absorption of radiation from a probing laser affect the properties of the medium under study. An estimate of such influence on the value of the Kerr constant is made. It is found that in the tip-plane system when using a ruby laser, the Kerr constant near the tip changes. The established dependence of the Kerr constant on the distance to the tip made it possible to obtain a calculated kerrogram that coincides with the experimental one. Thus, it is shown that the measuring instruments can influence the results obtained, that is, under certain conditions, the electro-optical research method is invasive. This fact should be taken into account when processing experimental kerrograms.

Key words: Kerr effect, breakdown of liquid dielectrics, pre-breakdown phenomena, invasiveness of the Kerr effect.
PACS number: 42.65.Hw.

1 Introduction

The role of experimental studies of pre-breakdown processes in liquid insulation, especially non-contact and non-invasive ones, cannot be overestimated. The study of fast processes, which previously manifested themselves significantly in liquids, became possible due to the development of high-speed optical methods that make it possible to reveal various processes using schlieren- and shadow photographs [1-4] , spectroscopic [5-8] and electro-optical methods [9-12]. Numerous experimental studies of pre-breakdown processes in dielectric liquids have shown that the nature of these processes differs significantly depending on the nature of the liquid, the length and configuration of the discharge gap, as well as the duration, polarity, amplitude of the applied voltage pulses, etc.

Of all the optical methods, the Kerr effect is the only one that provides a direct connection between the optical and electrical parameters of the object of study. However, the interpretation and interpretation of electro-optical measurements in optically active liquids is not only rather laborious but also must take into account various factors that arise and are not taken into account earlier. Any liquid makes an additional contribution to the modulation of the light beam associated with the configuration of the electric field and the value of the Kerr constant. As a result, the data obtained during the processing of experimental kerrograms do not always satisfy researchers.

The Kerr constant depends not only on the type of liquid [13] and on the wavelength of the probing radiation [14] but also on the liquid temperature [15]. Therefore, when studying with a laser and interpreting the results obtained, it is necessary, at least, to know the temperature distribution over the diagnosed zone and the reasons for its change. When using low-power lasers in uniform temperature and electric fields, no questions arise. The electro-optical method is indeed non-invasive, the Kerr constant justifies its name, and the research tool does not affect the object of study.

However, this is not always the case.

2 Methodology

The works [16] and [17] describe a series of electro-optical studies of the pre-breakdown stage of

the electrical breakdown of nitrobenzene. Due to the high labor intensity of the process of processing experimental data and the lack of adequate physical and mathematical models of the processes occurring in the near-electrode zone, a complete analysis has not been carried out. All data extracted from kerrograms in these works were obtained under the assumption that the method is invasive and the Kerr constant is unchanged.

To verify this statement, we took one of the experiments presented in [17] and [18] (see Fig. 1).

The kerrogram (see Fig. 1) was obtained at the pre-breakdown stage of nitrobenzene breakdown. The measuring cell was a quartz glass tube, into which specially prepared nitrobenzene was poured. The inner diameter of the tube is 15 mm. The electrode system consisted of a point with a radius of curvature of 0.3 mm and a plane with a diameter of 14 mm, made according to the Rogowski profile. The distance from the point to the plane is 30 mm. Stainless steel electrodes. Voltage 120 kV.

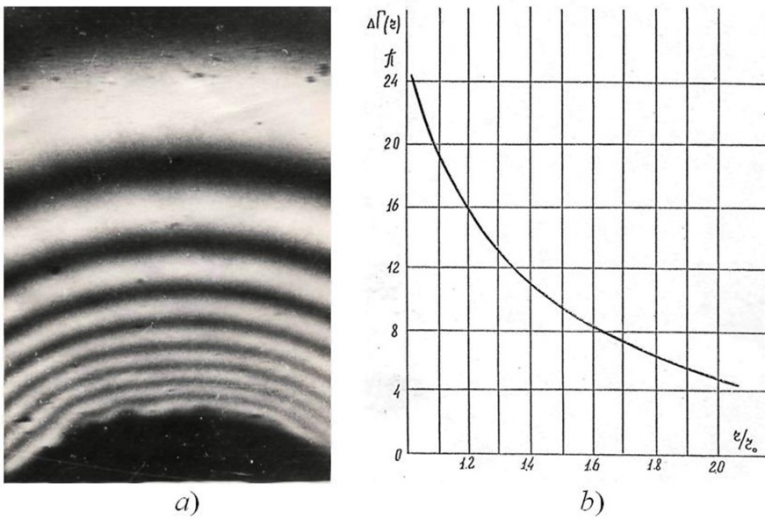

a) *b)*

Figure 1 – Distribution of Kerr bands near the tip-anode (*a*) and the phase shift distribution restored from it (*b*) along the axisymmetric electrode system; $z/r_0 = 1+z/r_0$ is the relative distance from the tip along the axis of symmetrical (r_0 is the radius curvature of the tip)

When studying pre-breakdown fields in polar liquids of the electro-optical Kerr effect, after the passage of a light beam through a polar dielectric in an electric field, the state of polarization of the probing radiation changes. The change in polarization can be converted into a change in the intensity of the transmitted light, for example, using an analyzer. In the case of crossed polarizer and analyzer oriented at an angle of 45° to the direction of the external field, the relative intensity of radiation after passing through the object is determined by the expression:

$$I/I_0 = \sin^2\left(\Delta\Phi/2\right) = \sin^2\left(2\pi \cdot B \cdot \ell \cdot E^2\right) \qquad (1)$$

Here I_0 and I are the intensity of the probing beam at the input and output from the Kerr cell, respectively, $\Delta\Phi$ is the phase shift; B is the Kerr constant; ℓ is the path length of the probing beam through the Kerr cell; E is the electric field strength.

The Kerr constant does not change, and the field strength E is assumed to be the same throughout the beam path, which is true only for rare cases.

The phase shift $\Delta\Phi$ is determined directly from the kerrogram, which is a picture of lines of the equal phase difference between the ordinary and extraordinary rays. Extracting information from experimental kerrograms is a rather ambiguous task. The fact is, the direction of the phase shift during decoding must be known a priori. In this way, a kerrogram is very similar to an interferogram when tuned to an infinitely wide band [18]. There is no such information in the kerrogram itself. Therefore, first of all, it is necessary to determine the reference band, for which the phase shift is known and close to zero, and then from it, calculate the phase shifts

for the remaining bands. Usually, the reference band is chosen in the region where there are no disturbances or they are very small. For a point-plane system, for example, this is a strip located far from the point. For other electrode systems, the situation is more ambiguous. If the reference band is determined incorrectly, then the results are not accurate, especially when the dimensions of the experimental kerrogram are insufficient.

The development of IT technologies and computer modeling methods has made it possible to take a new approach to the problem of restoring the physical properties of an object by analyzing experimentally obtained kerrograms.

Obtaining information about the electrical parameters of a liquid dielectric from the Kerr pattern is a rather complicated problem. Therefore, we have developed a method for deciphering kerrograms based on the most complete reproduction in a computer model of the geometric, physical, optical, and electrical conditions of a real experiment [19]. The criterion for the correctness of the computer model is the coincidence of the visualized results of the calculation with the real kerrogram.

The calculations were carried out by the finite element method in a 3D model of the measuring cell. The Z axis (Fig. 2) coincides with the direction of the electric field applied to the measuring cell.

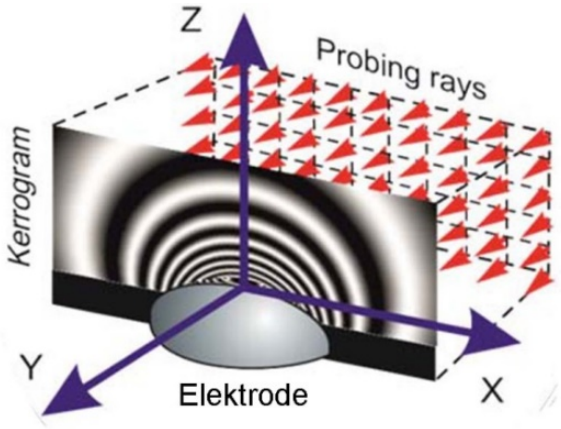

Figure 2 – Scheme of sounding during simulation

The electric field strength E was now determined as a function of the distance traveled by the beam through the measuring cell:

$$I(x,z)/I_0 = \sin^2\left(\pi \cdot B \cdot \int E_z^2(y)dy\right), \qquad (2)$$

where E_z is the projection of the electric field strength vector onto the Z axis.

Reproducing the experimental conditions from [16] as fully as possible, we obtained a calculated kerrogram, which we compared with the experimental one.

Fig. 3 shows the calculated and experimental kerrograms.

It can be seen that the kerrograms from Fig. 3 match only qualitatively. The simulation technique used by us made it possible to obtain the phase shift distribution $\Delta\Phi/\pi$, which made it possible to quantitatively compare our calculations with the results obtained after manual processing of the experimental kerrogram.

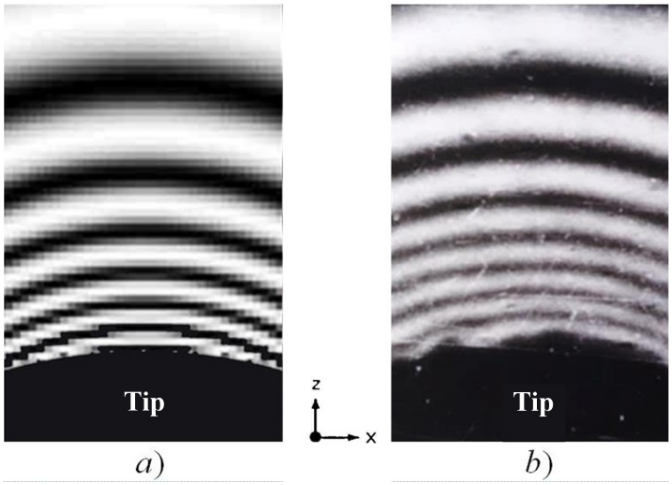

Figure 3 – Calculated (*a*) and experimental (*b*) kerrograms [7]

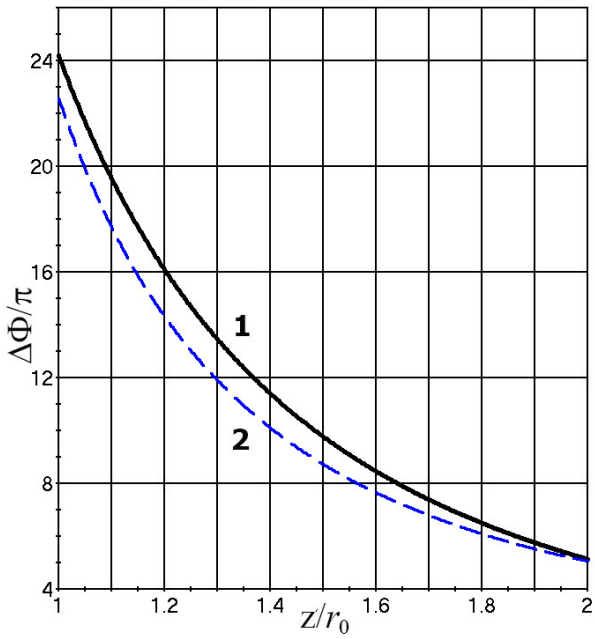

Figure 4 – Here 1 is an experimental (see fig 2) digitized curve ($\Delta\Phi/\pi_{min} \sim 5.10_{exp.}$), 2 is the calculated one ($\Delta\Phi/\pi_{min} = 5.06_{calc.}$), z/r_0 is the relative distance from the tip. Voltage 120 kV

Both curves are plotted for a constant $B = 3\times10^{-12}$ m/V^2. Since $\Delta\Phi/\pi = 2 \cdot B \cdot \ell \cdot E^2$, then a simple increase in the constant B will not bring the theoretical curve to the experimental one.

In our model

$$\frac{\Delta\Phi(y,z)}{\pi} = 2B(z) \cdot \int E_z^2(y,z)dy \qquad (3)$$

$$B(z) = \frac{\Delta\Phi(y,z)}{2\pi \cdot \int E_z^2(y,z)dy}. \qquad (4)$$

Digitization of the experimental curve and regression analysis gave the dependence

$$\Delta\Phi(y,z)/\pi = \frac{24{,}7645699}{(z/r_0)^{2{,}3286521}}. \qquad (5)$$

The integral $\int E_z^2(y,z)dy$ doesn't depend on B, therefore, from the joint solution of equations (4) and (5) by the numerical method for U = 120 kV, the dependence of B on z/r_0 was obtained:

$$B(z)_{120kV} = \frac{24{,}7645699}{(z/r_0)^{2{,}3286521} \cdot 2\int E_z^2(y,z)dy}. \quad (6)$$

The calculation of $\Delta\Phi/\pi = f(z/r_0)$ by the formula $\frac{\Delta\Phi(y,z)}{\pi} = 2B(z)_{120kV} \cdot \int E_z^2(y,z)dy$ gave a complete coincidence of the obtained curve with the experiment (see Fig. 2, curve 1). Thus, within the framework of our model, in order for the calculated results to coincide with the experimental data, it is necessary to admit the possible inconstancy of B.

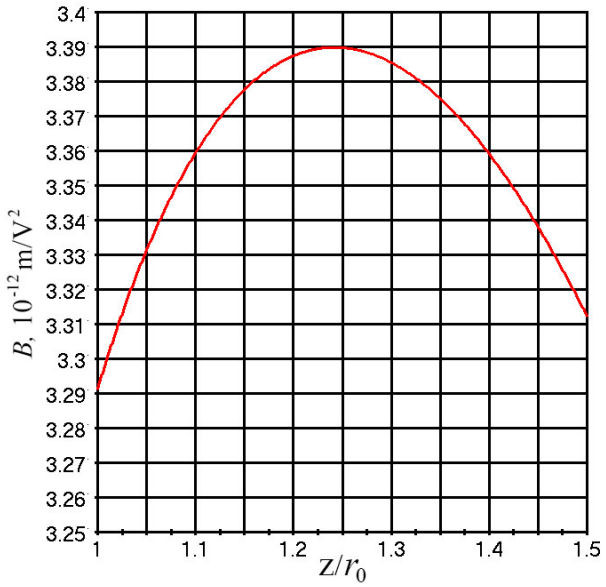

Figure 5 – Variation of the Kerr constant along the axis of symmetry

Therefore, it was necessary to look for the reason for such behavior of the Kerr constant.

But first, it was logical to see how the view of the calculated kerrogram changes, provided that B ≠ const. Following the algorithm proposed in [19], we obtained a new calculated kerrogram and compared it with the existing ones. The results of the comparison are shown in Fig. 6.

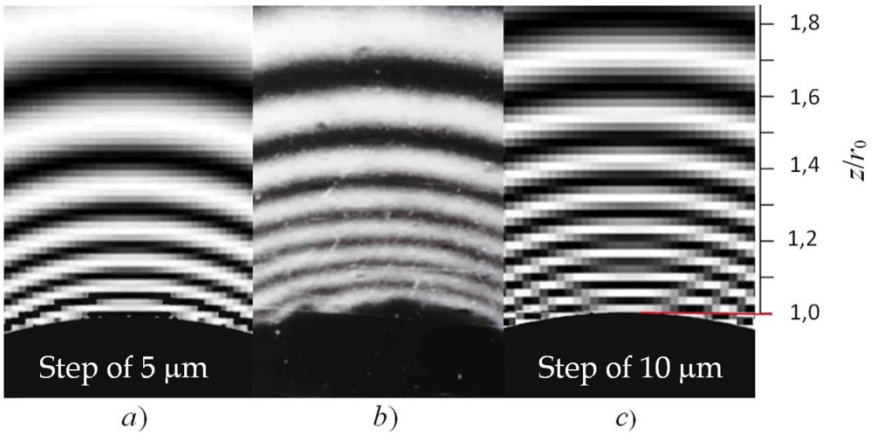

Figure 6 – Kerrograms: *a*) calculated, $B = 3.0\times10^{-12}$ m/V^2 [6]; *b*) experimental [4]; c) calculated, B is determined by formula (3) [8], p. 757]

If the left picture (Fig. 6*a*) at a constant Kerr constant practically does not coincide with the experimental one, then the right one (Fig. 6*c*), where $B = f\ (z/r_0)$, coincided quite well with the central one. Differences only in the upper part, starting from about 0.2 mm from the tip.

On the left kerrogram, the calculations were carried out with a step of 5 μm. The resulting picture has 50 calculated layers from the tip, that is, the height of the kerrogram is about 50×0.005 = 0.25 mm or $z/r_0 = 1.83$ from the tip.

All kerrograms are shown on the same scale. The calculation step on the right picture (Fig. 4 *c*) was 2 times larger — 10 μm, so the spatial resolution is somewhat worse there. However, it can be seen that the best match is observed up to about 0.2 mm ($z/r_0 = 1.65$) from the tip.

Of course, the question arises that as you move away from the tip up to z = 0.075 mm ($z/r_0 = 1.25$), the constant B increases (see Fig. 3), and then begins to decrease. The change is small and, perhaps, the whole point is in the numerical methods for obtaining functional dependencies. Maybe the reason is something else. But the very fact of the coincidence of the calculated kerrogram (Fig. 6*b*) with the variable $B = f\ (z, r_0)$ and the experimental one (Fig. 6c) gives hope that everything will become clear with time.

A good match of the images in the apical zone, if the variable *B* is used in the calculations, made us think about the reasons for this. This behavior of the Kerr constant is really strange and does not fit into the established ideas, but it happens, and in any case, one should at least try to explain the results. We have made this attempt.

3 Results and discussion

As the temperature *T* increases, the constant *B* decreases [15]. So, it was necessary to try to consider the possible reasons for the heating of nitrobenzene in the apical region.

3.1 Influence of laser radiation, conduction currents, and dielectric losses on the heating of nitrobenzene

Let us estimate the contribution of various processes (absorption of the energy of probing laser radiation; heating by conduction currents; dielectric losses), which can lead to a possible increase in temperature.

In the experiment [16], a ruby laser with a rod 120 mm long and 12 mm in diameter was used. The illuminator included two IFP-2000 flash lamps. The laser was switched to a quasi-continuous regime by selecting the resonator configuration and the power supply mode of the flash lamps of the pumping system with pulse duration of the almost constant intensity of ~300 μs. The Q-switching of the laser was passively using a KS-18 light filter. The duration of individual giant pulses was at the level of 50-80 ns with an interval of 1 to 40 μs between them.

The absorption of radiant energy can be estimated using the information on the absorption coefficient of nitrobenzene given in [18], the energy values in the laser pulse, and the geometry of the experiment.

At a ruby laser wavelength λ_{Rb} = 694.3 nm, the thermal absorption coefficient α_T is ~ 8% [21]. Then, at an energy of ~ 1.2 J in the laser pulse, W_{Rb} ~ 100.0 mJ is absorbed in the measuring cell at a distance of 15 mm. With a laser beam diameter of 3 mm, this corresponds to ≈ 0.95 mJ/mm^3 or 0.95 J/cm^3 for the entire time the light pulse passes through nitrobenzene.

During the measurements, an SFR-2M ultra-high-speed photo recorder was first spun up, which launched the laser. After the laser reached the quasi-continuous mode, a command was given through the delay lines to start the GIN-400 generator, and frame-by-frame shooting was performed.

The moment of the first enlightenment of the passive shutter on the KS-18 depends on the energy and stability of the laser. In addition, due to the partial burnout of the dye of the light filter after each clarification of the KS-18, the interval until the next clarification can also vary within fairly large limits.

Since there is no data on the synchronization accuracy of the beginning of generation and the moment of frame registration, for estimation it can be set equal to half the lifetime of laser radiation.

This means that we can assume that nitrobenzene in the cell will absorb energy equal to 0.48 J/cm^3.

Joule heat due to conduction currents [17] and *dielectric losses* [22] are estimated at ~ 1 J/cm^3. In total, we get ~ 1.5 J/cm^3.

Therefore, the temperature of nitrobenzene in the near-point zone due to radiative absorption and heating due to conduction currents and dielectric losses can rise, and *B* can change.

Let's evaluate this possibility:

Specific heat c = 1.43 kJ/(kg·K) =1.43·10^3 J/(kg·K)

Density ρ = 1.2 g/cm^3 = 1.2·10^3 kg/m^3.

Then if Q = 1.5 J, then 1 cm^3 of nitrobenzene will heat up to:

$$\Delta T_{(Q=1{,}48\ J)} = Q/[c\cdot\rho\cdot V)] = \\ = 1.5/[(1.43\cdot10^3)\times(1.2\cdot10^3)\times1\cdot10^6]\ K = 0.87\ K.$$

In [15], the temperature dependence of the Kerr constant was obtained:

$$B(T) = a_0 + a_1/T + a_2/T^2, \qquad (7)$$

where $a_0 = 6.556\times10^{-12}$ m/V^2, $a_1 = -5.610\times10^{-9}$ m/V$^{2.}$ and $a_2 = 1.379\times10^{-6}$ m/V^2.

The joint solution of equations (6) and (7) made it possible to determine the functional dependence of temperature in our discharge gap on the distance to the tip:

$$T(z/r_0) = b_0 + b_1\times(z/r_0) + b_2\times(z/r_0)^2 + \\ + b_3\times(z/r_0)^3 + b_4\times(z/r_0)^4 + b_5\times(z/r_0)^5. \qquad (8)$$

Here $b_0 = 839.5458731$ K: $b_1 = -1813.0400453$ K; $b_2 = 2381.7153097$ K: $b_3 = 1553.9419213$ K: $b_4 = 504.7691571$ K: $b_5 = -65.0502323$ K

The dependence obtained for the radius of curvature of the tip $r_0 = 0.3$ mm is shown in Fig. 7.

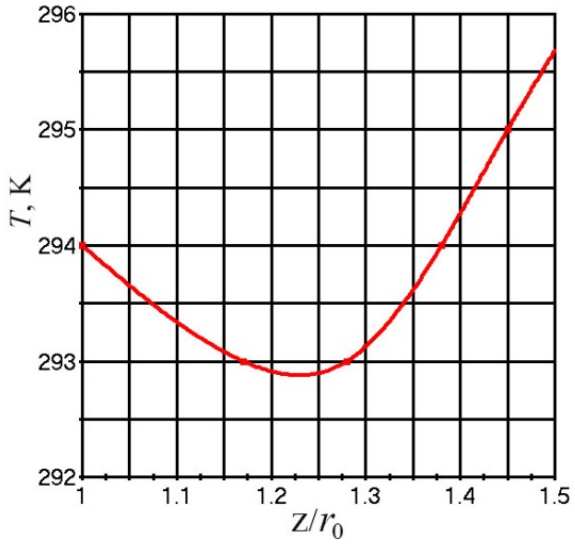

Figure 7 – Dependence of temperature on the coordinate $T = f(z/r_0)$

Graph from Fig. 7 correlates well with the graph in Fig. 5. The points at which $B = f_B(z/r_0)$ and $T = f_T(z/r_0)$ change are almost at the same distance from the tip with a radius of curvature of 0.3 mm ($z/r_0 = 1.25$ or z = 0.075 mm). Starting from this distance, the temperature rises approximately by $\Delta T_Q \sim 1.1$ K as it approaches the tip, which also does not differ much from the value obtained above $\Delta T_E \sim 0.87$ K

So, estimates show that the temperature can indeed increase by $\Delta T \approx 0.87$ K. According to the formula taken from [15], this gives a decrease in the Kerr constant by $\Delta B_T \sim 0.085\times10^{-12}$ m/V^2.

According to the schedule from Fig. 5, it turns out that $\Delta B_T \sim 0.096\times10^{-12}$ m/V^2. That is, the numbers correlate not only in order of magnitude. The discrepancy is due to the fact that the estimates of the absorbed energy were very approximate.

Therefore, an increase in temperature and a decrease in the Kerr constant in the near-point zone is, in principle, quite probable.

But rising temperatures are only one possible reason. Another reason is related to the behavior of a polar dielectric in a strong external field.

3.2 Influence of a strong electric field on the saturation of the polarization of nitrobenzene

In the point-plane system, the electric field, especially near the tip, is strongly inhomogeneous. In this case, the field strength values can reach such values that the probability of effects that are impossible or weakly manifested at lower fields increases. In particular, this concerns dipole saturation in polar liquids. Its essence lies in the predominant orientation of molecules along the field. As a result, after reaching certain field strength, with a further in-

crease in which the dipole moment per unit volume can no longer increase.

When an external electric field is applied in a polar dielectric, an optical axis is induced, which coincides in direction with the electric field strength vector. In this case, light propagates in the medium in the form of two waves: ordinary and extraordinary. The plane of polarization of the extraordinary wave coincides with the main plane, i.e. with a plane passing through the direction of propagation of the beam and the field vector, and the plane of polarization of an ordinary wave is perpendicular to it. In nitrobenzene, the refractive indices of ordinary n_o and extraordinary rays n_e depend on the magnitude of the external field:

$$n_o = n - \frac{1}{3}\lambda \cdot B \cdot E^2$$

and

$$n_e = n + \frac{2}{3}\lambda \cdot B \cdot E^2, \qquad (9)$$

where n is the refractive index in the absence of a field; λ is the wavelength of light; B is the Kerr constant, and E is the strength of the external field.

Expressions (9) are approximate and are obtained by expanding the dependence of the refractive index on the field $n(E) = n + \alpha \cdot E^2 + \beta \cdot E^4$ into a series, taking into account the terms containing E^2, and are valid when the following condition is met:

$$\lambda \cdot B \cdot E^2 << n .$$

It was suggested in [22] that the Kerr constant in nitrobenzene may also be affected by the occurrence of a state of saturation of the dipole polarization at $E \geq 1$ MV/cm. The related possible decrease in the Kerr constant $E << \sqrt{n/(\lambda \cdot B)}$ may well be present in the described experiments. On the other hand, in experiments [20] in the "blade-plane" and "point-plane" systems, it was proved that at intensities up to E = 1 MV/cm, the Kerr constant can be taken as a constant. Under the conditions of the experiment under consideration (see Fig. 2), the estimate of the field strength near the tip gives the value

$$E = 2U / [r_0 \, ln \, (4d/ r_0)] = 1{,}34 \text{ MV/cm}.$$

Here U and d are the voltage and the gap between the electrodes, and r_0 is the radius of curvature of the tip.

Consequently, according to this criterion, the condition for the occurrence of dipole saturation is satisfied. This leads to an increase in the field strength and a decrease in the Kerr constant near the tip.

4 Conclusions

Both considered mechanisms explaining the decrease in the Kerr constant near the tip in the tip-plane system are conjectural and require verification. But as versions, they have the right to exist.

In electro-optical studies, the experimental conditions can affect the value of the Kerr constant. If the laser is low power, the absorption of its energy can be ignored. If the fields are weak, the role of electrodynamics causes is negligible. That is, there will be neither heating nor saturation of polarization, and the Kerr constant remains unchanged.

Under the conditions considered by us, it turned out that it was in the point-plane system at the pre-breakdown stages of the development of nitrobenzene breakdown that the experimental and calculated kerrograms did not coincide. It was possible to bring them to coincidence only by allowing a change in the value of the Kerr constant.

Based on the analysis performed, it can be concluded that the electro-optical method of research using the Kerr effect cannot always be considered non-invasive. In certain situations, the measuring tool itself can change the conditions in the diagnosed object. Involuntarily, an analogy with the microworld arises when a measuring tool changes the conditions for the existence of the object of study. It turns out that under certain conditions, this possibility must be taken into account in the macrocosm as well.

References

1. Traldi E., Boselli M., et al. Schlieren imaging: a powerful tool for atmospheric plasma diagnostic // EPJ Techniques and Instrumentation. -2018. -Vol. 5. -P. 4. https://doi.org/10.1140/epjti/s40485-018-0045-1

2. Chadband W.G., Wright G.T. A pre-breakdown phenomenon in the liquid dielectric hexane // British Journal of Applied Physics. -1965. -Vol. 16(3). -P. 305–313.

3. Wong P., Forster E.O. High-speed schlieren studies of electrical breakdown in liquid hydrocarbons // Canadian Journal of Chemistry. -1977. -Vol. 55(11). -P. 1890–1898. https://doi.org/10.1139/v77-264

4. Seepersad Y., Pekker M., Shneider M. N., et al. Investigation of positive and negative modes of nanosecond pulsed discharge in water and electrostriction model of initiation // Journal of Physics D: Applied Physics. -2013. -Vol. 46. – P. 355201. https://doi.org/10.1088/0022-3727/46/35/355201

5. Frayssines P.E., Bonifaci N., Denat A., Lesaint O. Streamers in liquid nitrogen: characterization and spectroscopic determination of gaseous filament temperature and electron density // Journal of Physics D: Applied Physics. -2002. -Vol. 35. -P. 369–377. https://doi.org/10.1088/0022-3727/35/4/313

6. Frayssines P E, Bonifaci N., Lesaint O., Denat A. Spectroscopic investigation of positive filamentary streamers in liquid nitrogen // Proceedings of 17th Escampig. Constanta, Romania. – 2004. -P. 181–183.

7. Salazar J.N., Bonifaci N., Denat A., Lesaint O. Characterization and spectroscopic study of positive streamers in water. Proceedings of IEEE International Conference on Dielectric Liquids (ICDL). Coimbra, Portugal. -2005. -P. 89-92. https://doi.org/10.1109/ICDL.2005.1490034

8. Bårmann P., Kröll S., Sunesson A. Spectroscopic measurements of streamer filaments in electric breakdown in a dielectric liquid // Journal of Physics D: Applied Physics. -1996. -Vol. 29. -P. 1188–1196. https://doi.org/10.1088/0022-3727/29/5/012

9. Toker G., Bulatov V., Kovalchuk T., Schechter I. Micro-dynamics of optical breakdown in water induced by nanosecond laser pulses of 1064 nm wavelength // Chemical Physics Letters. -2009. -Vol. 471. -P. 244–248. https://doi.org/10.1016/j.cplett.2009.02.044

10. Kovalchuk T., Toker G., Bulatov V., Schechter I. Laser breakdown in alcohols and water induced by λ=1064 nm nanosecond pulses // Chemical Physics Letters. -2010. -Vol. 500. -P. 242–250. https://doi.org/10.1016/j.cplett.2010.09.076

11. Üstundag A., Zahn M. Comparative study of theoretical Kerr electro-optic fringe patterns in 2-D and axisymmetric electrode geometries // IEEE Transactions on Dielectrics and Electrical Insulation. -2001. -Vol. 8. -P.15–25. https://doi.org/10.1109/94.910422

12. Üstundag A., Gung T.J., Zahn M. Kerr electro-optic theory and measurements of electric fields with magnitude and direction varying along the light path // IEEE Transactions on Dielectrics and Electrical Insulation. -1998. -Vol. 5. -P. 421-442. https://doi.org/10.1109/94.689432

13. Izdebski M., Ledzion R. Kerr constant measurement technique for liquids exhibiting orientational ordering of molecules // Optik. -2017. -Vol. 140. -P. 812–822. https://doi.org/10.1016/j.ijleo.2017.05.014

14. Harrison N.J., Jennings B.R. Laser induced Kerr constants for pure liquids // Journal of Physical and Chemical Reference Data. -1992. -Vol. 21. -P. 157-163. https://doi.org/rg/10.1063/1.555911

15. Hebner R.E. Jr., Misakian M. Temperature dependence of the electro-optic Kerr coefficient of nitrobenzene // J. Appl. Phys. -1979. – Vol. 50. -No. 9. -P. 6016-6017. https://doi.org/10.1063/1.326675

16. Otchjot po nauchno issledovatel'skoj rabote «Issledovanie mehanizma impul'snogo elektricheskogo proboja poljarnyh zhidkih dijelektrikov». Tema: «Issledovanie putej povyshenija udel'noj zapasaemoj jenergii v vysokovol'tnyh impul'snyh nakopiteljah jenergii termojadernyh ustanovok». Nomer gosregistracii 78074914. SibNIIJe, Novosibirsk, 1980. (In Russian).

17. Ushakov V.Y., Klimkin V.F., Korobeynikov S.M. Impulse breakdown of liquids. Springer, Berlin, Germany. -2007, 397 p.

18. Yassinskiy V.B., Kuznetsova Yu.A. About Kerr`s fringes formation // Bulletin of L.N. Gumilyov ENU. Physics and Astronomy Series. – 2021. -Vol. 136. -No. 3. -P. 35-44. https://doi.org/10.32523/2616-6836-2021-136-3-35-44

19. Korobeynikov S.M., Kuznetsova Yu.A., Yassinskiy V.B. Simulation of electrooptical experiments in liquids // Journal of Electrostatics. -2020. -Vol. 106. -P. 103452. https://doi.org/10.1016/J.ELSTAT.2020.103452

20. Korobejnikov S.M., Kuznecova Ju.A., Yasinskij V.B. «Variacija postojannoj Kerra v nitrobenzole na predprobivnoj stadii v sisteme ostrijo-ploskost'» [Вариация постоянной Керра в нитробензоле на предпробивной стадии в системе остриё-плоскость] // Mezhdunarodnaja nauchno-prakticheskaja konferencija «Integracija nauki, obrazovanija i proizvodstva — osnova realizacii Plana nadir» (Saginovskie chtenija №12), 18-19 ijunja 2020 g. Chast' 1. C. 755-758. g. Karaganda. (In Russian).

21. Cabrera M.H., Marcano O.A., Ojeda A.J., Wetter N.U., Frejlich J. Absorption spectra of nitrobenzene measured with incoherent white-light excitation // AIP Conference Proceedings. – 2008. -P. 1183-1188. https://doi.org/10.1063/1.2926815

22. Rzoska, S. J., Zhelezny, V. P. (Eds.). Nonlinear Dielectric Phenomena in Complex Liquids. NATO Science Series II: Mathematics, Physics and Chemistry. (Springer, Berlin, Germany. -2005. 406 p. https://doi.org/10.1007/1-4020-2704-4